Synthesis, Characterization and Near-Infrared Photoluminescence of Monoporphyrinate Lanthanide Complexes Containing an Anionic Tripodal Ligand

Hongshan He,[a,c] Jianping Guo,[a] Zhixin Zhao,[a] Wai-Kwok Wong,*[a] Wai-Yeung Wong,[a] Wing-Kit Lo,[a] King-Fai Li,[b] Li Luo,[b] and Kok-Wai Cheah[b]

Keywords: Lanthanides / Photoluminescence / Porphyrins / Tripodal ligands

Twelve neutral stable complexes of ytterbium(III) and erbium(III) coordinated by anionic hydridotris(pyrazol-1-yl)borate and *meso*-tetraphenylporphyrinate, and its derivatives with different substituents in the *para* position of the phenyl groups, were prepared and characterized. Crystal structure analyses revealed that seven nitrogen atoms, four from the porphyrinate dianion and three from the anionic tripodal ligand, are symmetrically coordinated to the lanthanide ions. Photophysical investigations of the complexes showed an enhancement of near-infrared photoluminescence as compared to aqua-coordinated monoporphyrinate lanthanide complexes. The solvent effect and substituent effects on the photoluminescent properties of the complexes were also investigated

Introduction

Recently, near-infrared (NIR) photoluminescence of three lanthanide ions, Nd^{3+}, Er^{3+} and Yb^{3+}, has attracted considerable attention for their potential application in optical amplification and fluoroimmunoassay.[1−8] Direct excitation of lanthanide ions is difficult because of the forbidden nature of their electronic transitions.[9] However, indirect excitation of an organic chromophore (antenna) that interacts closely with lanthanide the ions can make the energy of the triplet state of the ligand transfer efficiently to the excited state of the lanthanide ion and enable the ion to emit light;[10] the design of molecular systems with binding ability and photosensitizing properties for the construction of efficient photoluminescent lanthanide complexes is the key issue of this active area of research. Porphyrins are good candidates for this purpose because they can form stable complexes with lanthanide ions and have high absorbance.[11−15]

Several reports on NIR photoluminescent studies of porphyrinate lanthanide complexes have appeared in the literature during the past decades.[7,16−19] The results with Yb^{3+} and Er^{3+} complexes revealed that the porphyrin could indeed absorb the light and transfer the energy to lanthanide ions. However, the limited structural variation of the complexes tends to prohibit intensive investigation of the photophysical properties of lanthanide complexes, because most of them were prepared by the direct interaction of lanthanide β-diketonates with free porphyrin bases in 1,3,5-trichlorobenzene.[11−17] The lanthanide ion was therefore always coordinated by one porphyrinate dianion and one β-diketonate anionic ligand, which was very difficult to remove. Recently, we established a new method for the preparation of cationic lanthanide porphyrinate complexes of the general formula $[Ln(Por)(H_2O)_3]Cl$ (Ln = Yb^{3+}, Er^{3+} and Y^{3+}), in which one porphyrinate dianion and three aqua molecules are coordinated to the lanthanide ion.[18−21] The three aqua ligands in $[Ln(Por)(H_2O)_3]Cl$ can be substituted easily by other ligands, for example the (cyclopentadienyl)tris(diethylphosphito)cobaltate(I) anion, to form stable complexes.[18] This provides an opportunity for us to modify the monoporphyrinate lanthanide complexes for photoluminescent studies.

In this paper, we report the synthesis and characterization of a series of new stable ytterbium(III) and erbium(III) porphyrinate complexes coordinated by another anionic tripodal ligand, namely hydridotris(pyrazol-1-yl)borate (Scheme 1). The crystallographic analyses showed that seven N atoms, four from the porphyrinate dianion and three from the anionic tripodal ligand, are coordinated to the metal ions. The photoluminescence of lanthanide com-

[a] Department of Chemistry, Hong Kong Baptist University
Waterloo Road, Kowloon Tong, Hong Kong, P. R. China
Fax: (internat.) + 852-3411-5862
E-mail: wkwong@hkbu.edu.hk
[b] Department of Physics, Hong Kong Baptist University
Waterloo Road, Kowloon Tong, Hong Kong, P. R. China
[c] Department of Applied Chemistry, National Huaqiao University
Quanzhou 362011, P. R. China
Supporting information for this article is available on the WWW under http://www.eurjic.org or from the author.

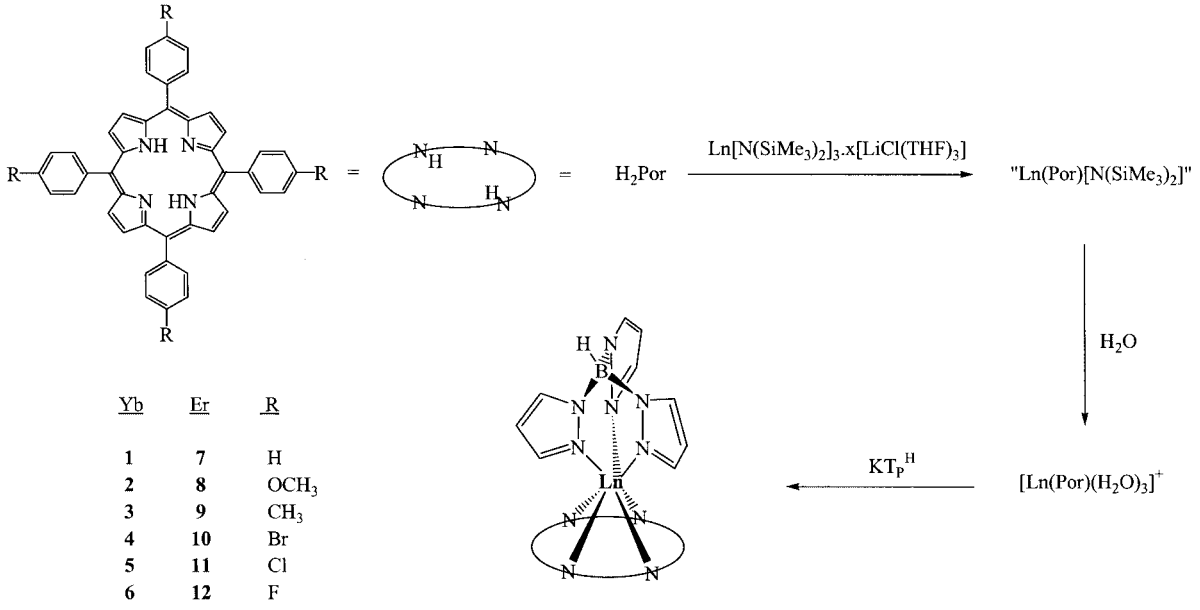

Yb	Er	R
1	**7**	H
2	**8**	OCH_3
3	**9**	CH_3
4	**10**	Br
5	**11**	Cl
6	**12**	F

Scheme 1

plexes was investigated in different solvents and the substituent effect on NIR luminescence will be discussed.

Results and Discussion

Synthesis and Characterization

The free porphyrin bases 5,10,15,20-tetraphenylporphyrin (H_2TPP), 5,10,15,20-tetrakis(*p*-tolyl)porphyrin (H_2TTP), 5,10,15,20-tetrakis(*p*-methoxyphenyl)porphyrin (H_2TMPP), 5,10,15,20-tetrakis(*p*-chlorophenyl)porphyrin (H_2TCPP), 5,10,15,20-tetrakis(*p*-bromophenyl)porphyrin (H_2TBPP), and 5,10,15,20-tetrakis(*p*-fluorophenyl)porphyrin (H_2TFPP), were prepared by direct condensation of the respective benzaldehyde with pyrrole in propionic acid according to the literature method[21] and purified by column chromatography using silica gel. The yields are 7−10%. Under a nitrogen atmosphere, refluxing of the free porphyrin base with a fivefold excess of $Ln[N(SiMe_3)_2]_3{\cdot}x[LiCl(THF)_3]$, generated in situ from the reaction of anhydrous $LnCl_3$ with three equivalents of $Li[N(SiMe_3)_2]$ in THF, in bis(2-methoxyethyl)ether for 48 h,[19−21] followed by stirring of the resulting mixture with a slight excess of potassium hydridotris(pyrazol-1-yl)borate (KT_p^H) in air at room temperature, gave the purple complexes $[Ln(Por)(T_p^H)]$ (Ln = Yb^{3+}, Por = TPP^{2-}, **1**; $TMPP^{2-}$, **2**; TTP^{2-}, **3**; $TBPP^{2-}$, **4**; $TCPP^{2-}$, **5** and $TFPP^{2-}$, **6**; Ln = Er^{3+}, Por = TPP^{2-}, **7**; $TMPP^{2-}$, **8**; TTP^{2-}, **9**; $TBPP^{2-}$, **10**; $TCPP^{2-}$, **11** and $TFPP^{2-}$, **12**) in high yields (Scheme 1). The complexes are quite stable in air and very soluble in chloroform, dichloromethane and *N*,*N*′-dimethylforamide. The electronic absorption spectra of complexes **1**−**12** are characteristic of normal metalloporphyrins.[23] The Soret band is observed at about 422 nm, while the Q bands are observed at 551 and 588 nm. After complexation, the number of Q bands of the porphyrin ring (four for free porphyrin base) is reduced to two. This is in agreement with Gouterman's four-orbital model,[24] which predicts that, due to an increase in symmetry, the four Q bands of the free porphyrin base will be reduced to two upon the formation of a metalloporphyrin. In the absorption spectra of regular metalloporphyrins there are two Q bands between 500 and 600 nm. The lower-energy band (α band) is the electronic origin Q(0,0) of the lowest singlet excited state S_1. The second band (β band) is its vibrational overtone and is labeled as Q(1,0). The relative intensities of these bands can be a qualitative yardstick of just how stable is the metal ion complexed to the four porphyrin nitrogen atoms. Thus, when the intensity of α is greater than that of β, the metal forms a stable complex with the porphyrin, whereas when α is less than β, the metal is easily displaced by protons.[25] The α/β relative intensity ratio for Yb^{3+} complexes **1**−**6** ranges from 0.12−0.44 and for Er^{3+} complexes **7**−**12** from 0.18−0.34. The typical N−H vibration for free porphyrin bases disappears from the IR spectra upon formation of the complexes. Complexes **1**−**12** exhibit similar fragmentation patterns in their mass spectra. Low-resolution (FAB-MS) and high-resolution mass spectra (ESI-HSMS) of the complexes confirmed that they are 1:1 adducts of monoporphyrinate and the anionic tripodal ligand. The electrospray ionization high-resolution mass spectra (positive mode) of the complexes in methanol show a mass peak corresponding to $[M + H]^+$. For instance, the Er^{3+} and Yb^{3+} complexes of $[Ln(TPP)(T_P^H)]$ exhibit mass peaks at m/z = 992.2815 and 1000.2788, respectively, which deviate by less than 5 ppm from the theoretical values of 992.2755 and 1000.2840 for the elemental composition of $C_{53}H_{39}BErN_{10}$ and $C_{53}H_{39}BN_{10}Yb$, respectively. The observed isotopic distribution patterns of the $[Ln(Por)(T_P^H) + H]^+$ peaks also match the expected theoretical signals.

Crystals of **1**·2$CHCl_3$, **5**·$CHCl_3$·CH_3OH and **7**·2$CHCl_3$ suitable for X-ray diffraction studies were grown by slow evaporation of the solvents from solutions of the respective compounds in a chloroform/methanol (v/v, 1:1) solution. Compounds **1**, **5** and **7** are isomorphous and crystallized in the monoclinic space group $P2_1/n$ for **1** and **7**, and $P2_1/c$ for **5**. The selected bond lengths and bond angles of the complexes are given in the Supporting Information (Table S1). Perspective drawings of compounds **1** and **7** are shown in Figure 1 and 2, respectively. The structural analyses revealed that the lanthanide(III) ions are seven coordinate, surrounded by seven nitrogen atoms, four from the porphyrin dianion and three from the anionic tripodal ligand. The average bond length of Ln−N(porphyrin) is shorter than that of Ln−N(tripodal ligand), with Ln−N(porphyrin) and Ln−N(tripodal ligand) being 2.356 and 2.495 Å for **1**, 2.357 and 2.508 Å for **5**, and 2.373 and 2.518 Å for **7**, respectively.

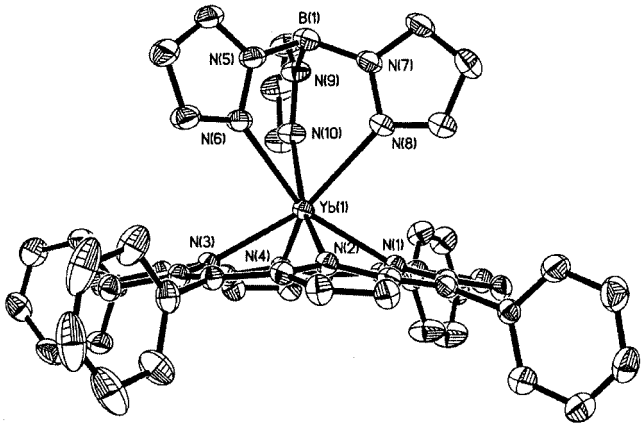

(a)

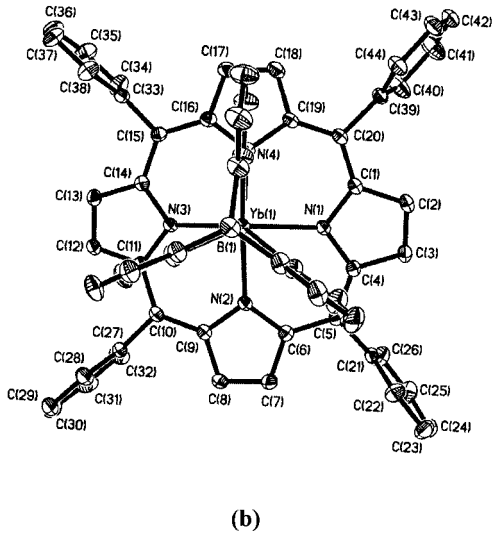

(b)

Figure 1. Perspective views of complex **1**: (a) side view; (b) top view

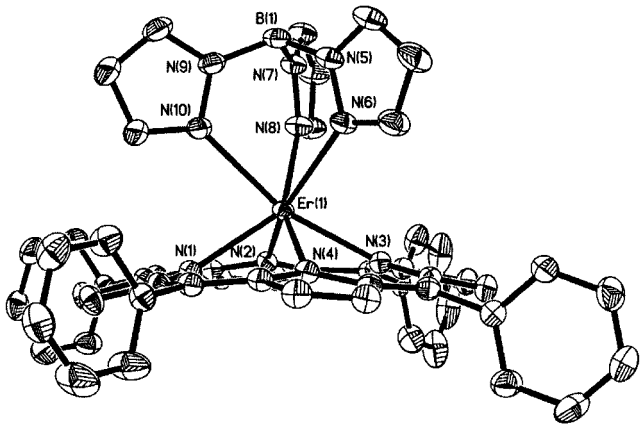

(a)

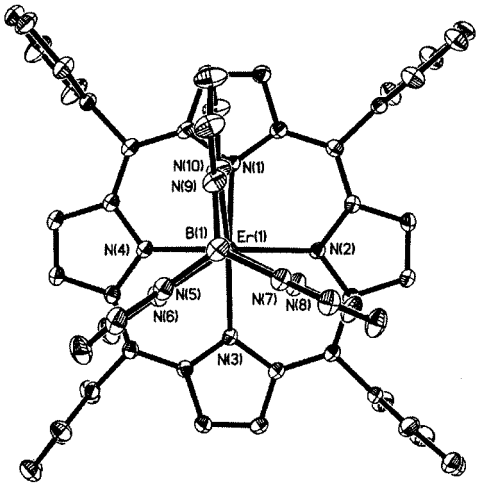

(b)

Figure 2. Perspective views of complex **7**: (a) side view; (b) top view

The mean nitrogen plane ($N_1N_2N_3N_4$) of the porphyrin dianion is almost parallel to the mean nitrogen plane ($N_6N_8N_{10}$) of the anionic tripodal ligand, forming a dihedral angle of 0.4°, 2.0° and 0.3° for **1**, **5** and **7**, respectively. The distance of the metal ion to the $N_1N_2N_3N_4$ mean plane is 1.172 Å for **1**, 1.167 Å for **5** and 1.195 Å for **7**, which is longer than that for [Ln(Por)$(H_2O)_3$]Cl[20] and shorter than that for [Ln(Por)(L_{OEt})] [L_{OEt} = cyclopentadienyltris(diethylphosphito)cobaltate(I)].[18] The distance of the metal ion to the $N_6N_8N_{10}$ mean plane is about 0.6 Å longer than that to the $N_1N_2N_3N_4$ mean plane, so the metal ion is much closer to the $N_1N_2N_3N_4$ mean plane. The substituents have little effect on the structural parameters except that the electron-withdrawing group (Cl) on the phenyl group gives a larger dihedral angle between the two planes (Table 1). The relative conformation of the tripodal ligand and the porphyrin dianion is slightly different between the Yb^{3+} and Er^{3+} complexes. A top view of their

structures reveals that, for the Yb^{3+} complexes, one of the pyrazole planes of the tripodal ligand is just above one of the phenyl groups of the porphyrin dianion, while the other two pyrazole groups are above the pyrrole groups; for the Er^{3+} complex, all the three pyrazole groups are located above the pyrrole groups.

Table 1. Distance from the metal ion to the $N_1N_2N_3N_4$ and $N_6N_8N_{10}$ planes

Compound	d_1[a] (Å)	d_2[b] (Å)	A[c] (°)	Ref.
1	1.172	1.780	0.4	this work
5	1.167	1.790	2.0	this work
[Yb(TMPP)(H_2O)$_3$]Cl	1.08			[20]
7	1.195	1.800	0.3	this work
[Er(TMPP)(H_2O)$_3$]Cl	1.11			[20]
[Er(TPP)(L_{OEt})]	1.201			[18]

[a] Distance to the $N_1N_2N_3N_4$ mean plane. [b] Distance to the $N_6N_8N_{10}$ mean plane. [c] Dihedral angle formed between the $N_1N_2N_3N_4$ mean plane and the $N_6N_8N_{10}$ mean plane.

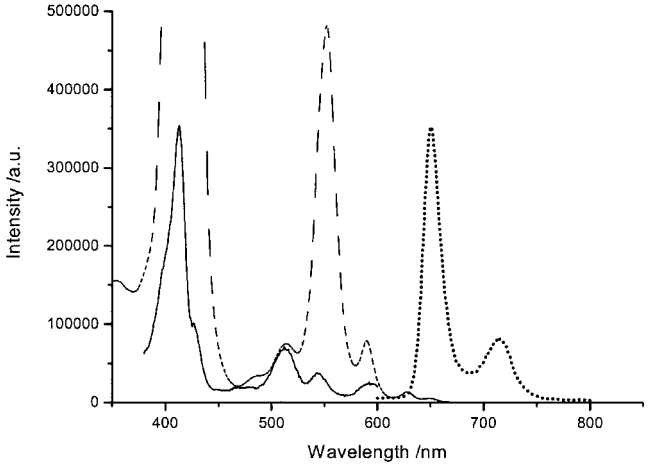

Figure 3. Room temperature absorption (– – –), emission (·····) (excited at 414 nm) and excitation (——) (monitored at 648 nm) spectra of **1** in $CHCl_3$

Photoluminescence Studies

The photophysical properties of compounds **1**−**12** were examined and the data are summarized in Table 2. The room temperature solution electronic absorption, excitation and emission spectra of compounds **1**−**12** in the UV/Vis region are almost identical and are characteristic of intra-ligand transitions of normal porphyrinate complexes.[13] Figure 3 shows the absorption, emission (excited at 414 nm) and excitation (monitored at 648 nm) spectra of **1**. The absorption bands at 421, 550 and 588 nm and emission peaks at 648 nm (τ = 12.9 ns and $\Phi_{em} = 0.11 \times 10^{-3}$) can be assigned to the intra-ligand $\pi \rightarrow \pi^*$ transitions of the porphyrinate ligand. The quantum efficiency of the metalloporphyrin is much lower than that of the corresponding free porphyrin base. For example, the quantum yield of **1** is less than 1% of the corresponding free porphyrin base H_2TMPP ($\Phi_{em} = 2.84 \times 10^{-2}$). Other than the visible emission, compounds **1**−**12** also exhibit typical emission corresponding to the lanthanide(III) ion in the near-infrared (NIR) region. Figure 4 shows the NIR emission and the excitation spectrum of **1**. The excitation bands of **1** in chloroform solution at 298 K (monitored at 980 nm) are observed at 560 and 596 nm, which almost coincide with its visible absorption bands at 550 and 588 nm. This clearly shows that the excitation of the Yb^{3+} ion is due to the $\pi \rightarrow \pi^*$ transitions of the porphyrinate antenna and excitation of the porphyrin is the photophysical pathway leading to the observable NIR luminescence. This is in agreement with our previous photoluminescent studies on related lanthanide porphyrinate complexes,[18,23] which show that the porphyrinate antenna transfers its absorbed visible energy of the Q band to the excited state of the metal ion, which then relaxes through emission in the NIR region. The NIR luminescence lifetime of **1**−**6** is about 20 μs and is much longer than the lifetime of the porphyrinate emission. Due to the limitation of our

Table 2. Photophysical data of compounds **1**−**12**[a]

Compound	Absorption: λ_{max}/nm [log(ε/dm^3 mol^{-1} cm^{-1})]	Excitation: λ_{exc}/nm	Emission: λ_{em}/nm (τ, $\Phi_{em} \times 10^3$)[b][c]
1	421 (5.55), 550 (4.15), 588 (3.22)	414	648 (12.9 ns, 0.11), 980 (20 μs)
2	424 (5.46), 552 (4.15), 592 (3.79)	418	647 (12.7 ns, 22.8), 980 (20 μs)
3	423 (5.58), 552 (4.23), 590 (3.87)	418	650 (13.2 ns, 0.22), 980 (20 μs)
4	423 (5.59), 551 (4.25), 588 (3.46)	417	650 (12.6 ns, 0.04), 980 (20 μs)
5	422 (5.62), 551 (4.27), 589 (3.48)	417	649 (12.4 ns, 0.31), 980 (20 μs)
6	421 (5.60), 550 (4.23), 587 (3.33)	415	650 (12.8 ns, 0.57), 980 (20 μs)
7	423 (5.72), 552 (4.31), 590 (3.57)	414	648 (9.1 ns, 0.16), 1540[d]
8	427 (5.52), 555 (4.14), 593 (3.67)	419	655 (9.1 ns, 0.03), 1540
9	424 (5.71), 553 (4.32), 592 (3.74)	418	651 (10.7 ns, 0.20), 1540
10	423 (5.63), 552 (4.18), 590 (3.48)	417	650 (10.5 ns, 0.26), 1540
11	424 (5.69), 552 (4.28), 590 (3.53)	416	650 (11.8 ns, 0.06), 1540
12	423 (5.63), 552 (4.22), 589 (3.49)	414	648 (11.7 ns, 0.17), 1540

[a] Photophysical measurements were made in $CHCl_3$ solution at room temperature. [b] Quantum yields were determined relative to [Ru(bipy)$_3$]Cl$_2$ in air-equilibrated water (Φ = 0.028). [c] Due to the limitation of the instrument, we were unable to determine the quantum yields of the NIR luminescence of compounds **1**−**12**. [d] Due to the limitation of the instrument, we were unable to measure the lifetime of the NIR luminescence of compounds **7**−**12**.

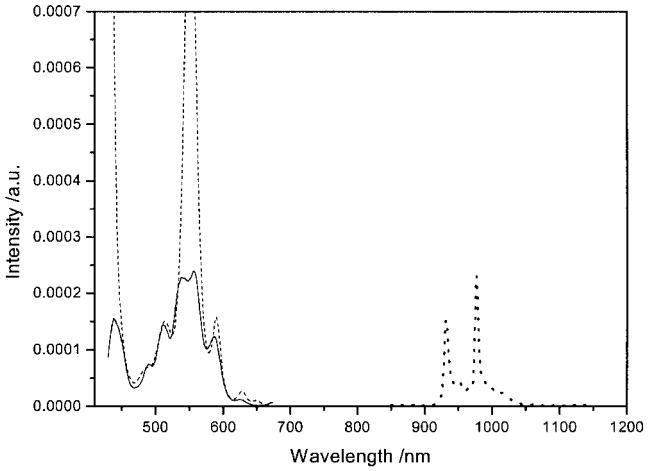

Figure 4. Room temperature absorption (– – –), NIR emission (·····) (excited at 420 nm) and excitation (——) (monitored at 980 nm) spectra of **1** in $CHCl_3$

equipment, we were unable to measure the excitation (monitored at 1540 nm) spectrum and the NIR luminescence lifetime of **7**–**12**.

The NIR emission spectra of the porphyrinate complexes are depicted in Figure 5. For the Yb^{3+} complexes, a strong emission due to the $^2F_{5/2} \rightarrow {}^2F_{7/2}$ transition is observed at 997 nm. This transition is split into six bands, one of these is sharp (980 nm) and the other five are weak (934, 953, 1002, 1020 and 1038 nm).For the Er^{3+} counterparts, two major peaks centered at 1018 and 1570 nm are observed. These can be attributed to the $^4I_{11/2} \rightarrow {}^4I_{15/2}$ and $^4I_{13/2} \rightarrow {}^4I_{15/2}$ transitions respectively. The first peak (1018 nm) splits into two others at 984 and 1020 nm, and the second peak (1570 nm) splits into five others at 1502, 1540, 1570, 1608 and 1634 nm.[2,4,8] The intensity of the emission of the complexes is enhanced relative to the aqua-coordinated monoporphyrinate complexes $[Ln(Por)(H_2O)_3]Cl$, as shown in Figure 6. Previously, we have investigated the photoluminescent properties of Yb^{3+} porphyrinate coordinated by L^-_{OEt}.[7] Well-split NIR emission peaks are also observed due to the strong bonding of the ligand to the Yb^{3+} ion. The present work further demonstrates that, upon coordination, the anionic tripodal ligand removes the degeneracy of the energy levels of the lanthanide ions by lowering the symmetry of these ions.

Figure 7 shows a simple, widely accepted photophysical model for the description of the sensitization process.[4,8] In this process, the porphyrin absorbs the light and is excited to its singlet state (S_1). The energy is then transferred to its triplet state (T_1), which is, in part, being transferred to the excited state of the lanthanide ion $(Ln^{3+})^*$ to produce the final luminescence. The overall NIR luminescence quantum yield (Φ) of the metal ion is the product of triplet yield (Φ_{ISC}), energy-transfer yield (Φ_{ET}) and the intrinsic luminescence quantum yield of the lanthanide ion (Φ_{Ln}). The structural and electronic variation of the porphyrin can disturb the excited energy level of the complexes and thus change the emission properties.[26,27] Therefore, we measured the NIR photoluminescence intensity of the complexes with different substituents in the *para* position of the phenyl groups of the porphyrin and found that both electron-do-

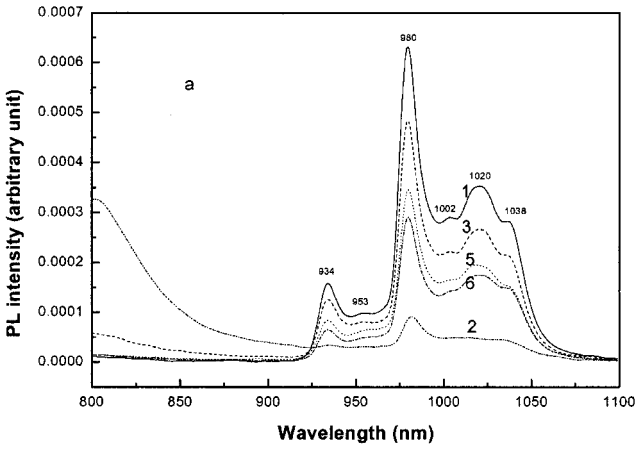

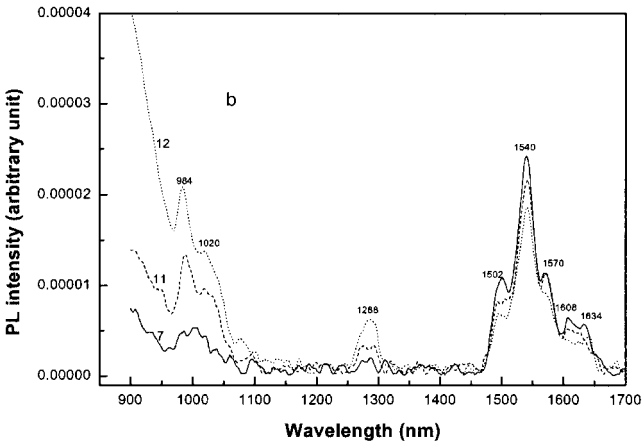

Figure 5. Luminescence of different (a) Yb^{3+} and (b) Er^{3+} complexes in chloroform at room temperature

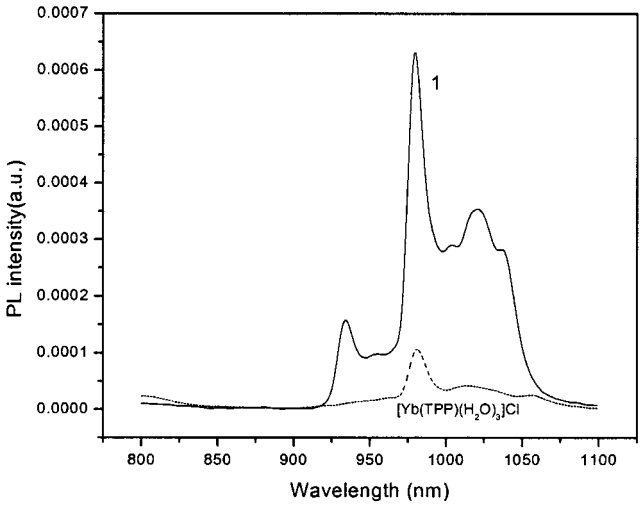

Figure 6. Luminescence of complex **1** and $[Yb(TPP)(H_2O)_3]Cl$ in chloroform at room temperature

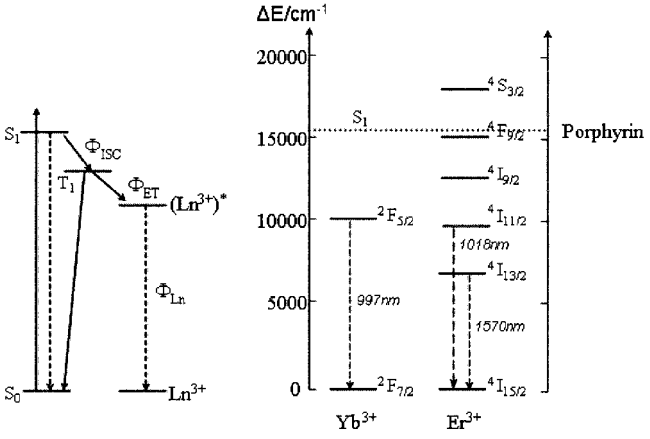

Figure 7. Schematic energy diagram of [Ln(Por)(T_p^H)] complexes; the arrows indicate the excitation mechanism of lanthanide ions by the porphyrin sensitizer ($S_0 \rightarrow S_1$ transition followed by intersystem crossing and energy transfer)

nating groups and halogen atoms are unfavorable for the NIR emission of Yb^{3+} complexes. For example, the unsubstituted complex **1** gave the strongest emission, with an intensity about six times higher than that of complex **2** and twice that of **6**. The reason for this is that electron donating groups (-OCH_3, -CH_3, etc.) allow the electrons on the phenyl groups to show greater π-conjugation with the porphyrin ring in the S_1 state, which results in an increase of the fluorescence quantum yield of the ligand and a decrease of the quantum yield of intersystem crossing Φ_{ISC}. Furthermore, the halogens can decrease the rate of intersystem crossing and thus make the Φ_{ISC} quite low.[26,28,29] The lower Φ_{ISC} leads to a weaker metal ion emission. As the emission of Er^{3+} complexes is much lower than that of Yb^{3+} complexes, the substituent effect was not apparent here.

We have also investigated the NIR photoluminescence of complex **7** in different solvents (Figure 8). The results showed that the NIR emission intensity of **7** is strongest in non-polar solvents such as benzene, gradually decreases as the polarity of the solvent increases and is completely quenched in methanol. According to the theory of non-radiative transitions in lanthanide complexes, the non-radiative relaxation between various J states may occur by interaction of the electronic levels of the lanthanide ion with suitable vibrational modes of the environment.[30] The presence of OH groups in methanol enhances the non-radiative deactivation of the lanthanide ion by vibronic coupling with the vibrational states of the O−H oscillators and thus quenches the emission.[31]

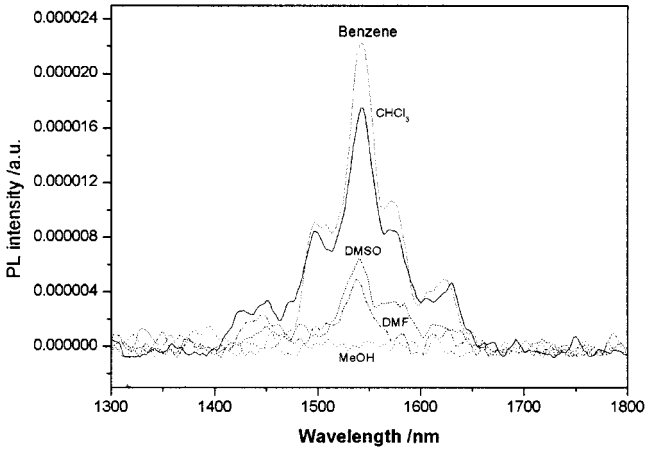

Figure 8. Luminescence of complex **7** in different solvents at room temperature

Concluding Remarks

In this paper, we have reported the synthesis of a series of lanthanide porphyrinate complexes of the general formula [Ln(Por)(T_P^H)] by the interaction of cationic porphyrinate complexes [Ln(Por)$(H_2O)_3$]Cl, generated in situ, with anhydrous KT_P^H and demonstrated that these complexes are good precursors for the preparation of other lanthanide porphyrinate complexes. We have also shown that porphyrinate ligands can behave as antennae by absorbing visible light and thus sensitize the NIR emission of lanthanide ions. Electron-donating groups and halogen atoms on the phenyl groups of the porphyrin ring are unfavorable for the emission of lanthanide ions.

Experimental Section

General: All reactions were carried out under an atmosphere of dry nitrogen. Solvents were dried by standard procedures, distilled and deaerated prior to use. All chemicals used were obtained from Aldrich Chemical Company. 5,10,15,20-Tetraphenylporphyrin (H_2TPP), 5,10,15,20-tetrakis(*p*-tolyl)porphyrin (H_2TTP), 5,10,15,20-tetrakis(*p*-methoxyphenyl)porphyrin (H_2TMPP), 5,10,15,20-tetrakis(*p*-chlorophenyl)porphyrin (H_2TCPP), 5,10,15,20-tetrakis(*p*-bromophenyl)porphyrin (H_2TBPP), 5,10,15,20-tetrakis(*p*-fluorophenyl)porphyrin (H_2TFPP) were prepared according to the literature methods by condensation of pyrrole and the corresponding aldehyde,[22] and characterized by TLC, ^{1}H NMR spectroscopy and FAB mass spectrometry. The IR spectra (KBr pellets) were recorded on a Nicolet Nagba-IR 550 spectrometer. NMR spectra were recorded on a Varian INOVA 400 spectrometer. Low-resolution mass spectra were obtained on a Finnigan MAT SSQ-710 in FAB (positive) mode. Electrospray ionization high-resolution mass spectra (ESI-HRMS) were recorded on a QSTAR mass spectrometer. Electronic absorption spectra in the UV/Vis region were recorded on a Hewlett−Packard 8453 UV/Visible Spectrophotometer, steady-state visible fluorescence and PL excitation spectra on a Photon Technology International (PTI) Alphascan spectro-fluorimeter and visible decay spectra on a pico-N_2 laser system (PTI Time Master) with λ_{exc} = 337 nm. NIR emission was detected by a liquid-nitrogen-cooled InSb IR detector (EG & G) with a preamplifier and recorded by a lock-in amplifier system as the third harmonic; the 355 nm line of an Nd:YAG laser (Quantel Brilliant B) was used as excitation light and also to pump the OPO (Opotek MagicPrism VIR) to provide a continuously tunable laser source from 410−670 nm with a pulse-width of 4 ns. NIR decay spectra were detected by an Oriel 77343 photomultiplier and monitored by a HP54522A 500 MHz oscilloscope. Quantum yields were computed according to the literature method[32] using [Ru(bipy)$_3$]Cl_2 as the reference standard (Φ = 0.028 in air-equilibrated

water).[33] To avoid any second-order light reaching the detector, 710 and 830 nm cutoff filters were used where applicable. The complexes in different solution were analyzed in quartz cells at a concentration of 2×10^{-5} M. The power on the cell was 1 W and all spectra were corrected for the detector response.

Preparations of Precursor Complexes: Stock solutions of the precursor complexes, $Ln[N(SiMe_3)_2]_3{\cdot}x[LiCl(THF)_3]$ (Ln = Yb^{3+} and Er^{3+}), were prepared in a similar manner. A detailed description is given for the Yb^{3+} complex.

$Yb[N(SiMe_3)_2]_3{\cdot}x[LiCl(THF)_3]$ Solution (Solution A): *n*BuLi (31.0 mL, 1.6 M in hexane, 49.6 mmol) was added slowly over a period of 30 min to a solution of $(Me_3Si)_2NH$ (10.8 mL, 8.26 g, 51.2 mmol) in THF (20 mL) cooled in an ice bath. The reaction mixture was stirred, warmed up slowly to room temperature and stirred for another 12 h until a clear pale yellow solution was obtained. Then, the resultant solution was transferred slowly to a suspension of $YbCl_3$ (4.45 g, 15.9 mmol) in THF (20 mL). The reaction mixture was stirred for 24 h at room temperature until all of the $YbCl_3$ had been consumed. The resulting solution was centrifuged, filtered and the filtrate was made up to 100 mL with THF to give an approximately 0.16 M solution of $Yb[N(SiMe_3)_2]_3{\cdot}x[LiCl(THF)_3]$ (solution **A**).

$Er[N(SiMe_3)_2]_3{\cdot}x[LiCl(THF)_3]$ Solution (Solution B): The procedure for the preparation of solution **B** was the same as for solution **A**. *n*BuLi (15.5 mL, 1.6 M in hexane, 24.8 mmol), $(Me_3Si)_2NH$ (5.4 mL, 4.13 g, 25.6 mmol) and $ErCl_3$ (2.18 g, 8.0 mmol) were used. The resulting solution was then made up to 50 mL with THF to give an approximately 0.16 M solution of $Er[N(SiMe_3)_2]_3{\cdot}x[LiCl(THF)_3]$ (solution **B**).

Preparations of Compounds 1−12: Compounds **1**−**12** were prepared by the same procedure. A typical procedure is given for **1**.

[Yb(TPP)(Tp^H)] (1): Solution **A** (5.0 mL) was added to a solution of H_2TPP (0.10 g, 0.16 mmol) in bis(2-methoxyethyl)ether (6 mL) under a nitrogen atmosphere. The resulting solution was refluxed and the progress of the reaction was monitored by UV/Vis absorption spectroscopy until most of the free base had coordinated to the metal ion. Then, anhydrous KT^H_P (0.10 g, 0.40 mmol) was added and the resulting mixture was stirred in air for another 12 h. After the reaction was complete, the solvent was removed in vacuo and the residue redissolved in chloroform, filtered and chromatographed on silica gel using chloroform to elute the unchanged free porphyrin base first, and then chloroform/methanol (v/v, 10:1) to elute the product. The solvent was removed on a rotary evaporator. The product was dissolved in chloroform (5 mL) and the solution was filtered. Diffusion of methanol into the chloroform solution gave purple crystals of the desired complex. Yield: 0.14 g (87%). M.p. > 300 °C. IR (KBr): $\tilde{\nu}$ = 3420 m, 2965 m, 2453 w, 1159 m, 1439 m, 1331 s, 1263 s, 1201 m, 1048 s, 988 vs, 798 vs, 751 s, 700 s cm^{-1}. MS (+FAB): *m*/*z* = 999 $[M + H]^+$, 786 $[Yb(TPP)]^+$ for ^{174}Yb. ESI-HRMS (+ve mode, in CH_3OH): *m*/*z* = 1000.2788 {$[M + H]^+$, $C_{53}H_{39}BN_{10}Yb$ requires 1000.2840}.

[Yb(TMPP)(Tp^H)] (2): Solution **A** (5.0 mL), H_2TMPP (0.11 g, 0.16 mmol) and KT^H_P (0.10 g, 0.40 mmol) were used. Yield: 0.18 g (89%). M.p. > 300 °C. IR (KBr): $\tilde{\nu}$ = 3441 m, 2924 m, 2831 w, 1605 s, 1512 s, 1466 m, 1290 s, 1243 vs, 1171 vs, 1036 m, 1000 w, 798 m, 742 w, 607w cm^{-1}. MS (+FAB): *m*/*z* = 1121 $[M + H]^+$, 906 $[Yb(TMPP)]^+$ for ^{174}Yb. ESI-HRMS (+ve mode, in CH_3OH): *m*/*z* = 1120.3259 {$[M + H]^+$, $C_{57}H_{47}BN_{10}O_4Yb$ requires 1120.3263}.

[Yb(TTP)(Tp^H)] (3): Solution **A** (5.0 mL), H_2TTP (0.10 g, 0.16 mmol) and KT^H_P (0.10 g, 0.40 mmol) were used. Yield: 0.13 g (80%). M.p. > 300 °C. IR (KBr): $\tilde{\nu}$ = 3449 s, 2918 w, 2459 w, 1641 m, 1512 m, 1409 m, 1331 s, 1294 m, 1124 vs, 1059 s, 991 vs, 801 s, 762 s, 731 s cm^{-1}. MS (+FAB): *m*/*z* = 1056 $[M + H]^+$, 842 $[Yb(TTP)]^+$ for ^{174}Yb. ESI-HRMS (+ve mode, in CH_3OH): *m*/*z* = 1055.3377 {$[M + H]^+$, $C_{57}H_{46}BN_{10}Yb$ requires 1055.3388}.

[Yb(TBPP)(Tp^H)] (4): Solution **A** (5.0 mL), H_2TBPP (0.13 g, 0.14 mmol) and KT^H_P (0.10 g, 0.40 mmol) were used. Yield: 0.16 g (90%). M.p. > 300 °C. IR (KBr): $\tilde{\nu}$ = 3415 s, 2919 m, 2448 w, 1641 m, 1479 m, 1393 m, 1331 s, 1196 s, 1070 m, 1049 s, 990 vs, 799 vs, 725 m, 462 m cm^{-1}. MS (FAB, +ve): *m*/*z* = 1312 $[M + H]^+$, 1098 $[Yb(TBPP)]^+$ for ^{79}Br and ^{174}Yb. ESI-HRMS (+ve mode, in CH_3OH): *m*/*z* = 1311.9138 {$[M + H]^+$, $C_{53}H_{35}BN_{10}Br_4Yb$ requires 1311.9261}.

[Yb(TCPP)(Tp^H)] (5): Solution **A** (5.0 mL), H_2TCPP (0.10 g, 0.14 mmol) and KT^H_P (0.10 g, 0.40 mmol) were used. Yield: 0.12 g (81%). M.p. > 300 °C. IR (KBr): $\tilde{\nu}$ = 3420 m, 2918 w, 2459 m, 1641 m, 1479 s, 1387 m, 1331 s, 1212 m, 1090 s, 1048 s, 990 vs, 801 s, 760 m, 725 m, 496 m cm^{-1}. MS (+FAB): *m*/*z* = 1136 $[M + H]^+$, 922 $[Yb(TCPP)]^+$ for ^{35}Cl and ^{174}Yb. ESI-HRMS (+ve mode, in CH_3OH): *m*/*z* = 1138.1247 {$[M + H]^+$, $C_{53}H_{35}BN_{10}Cl_4Yb$ requires 1138.1267}.

[Yb(TFPP)(Tp^H)] (6): Solution **A** (5.0 mL), H_2TFPP (0.11 g, 0.17 mmol) and KT^H_P (0.10 g, 0.40 mmol) were used. Yield: 0.13 g (78%). M.p. > 300 °C. IR (KBr): $\tilde{\nu}$ = 3426 m, 2924 m, 2458 w, 1600 m, 1517 vs, 1520 vs, 1485 m, 1408 m, 1329 m, 1226 s, 1157 vs, 1048 s, 991 s, 804 vs, 726 m, 591 m, 534 m cm^{-1}. MS (FAB, +ve): *m*/*z* = 1072 $[M + H]^+$, 858 $[Yb(TFPP)]^+$ for ^{174}Yb. ESI-HRMS (+ve mode, in CH_3OH): *m*/*z* = 1072.2526 {$[M + H]^+$, $C_{53}H_{35}BN_{10}F_5Yb$ requires 1072.2464}.

[Er(TPP)(Tp^H)] (7): Solution **B** (5.0 mL), H_2TPP (0.10 g, 0.16 mmol) and KT^H_P (0.10 g, 0.40 mmol) were used. Yield: 0.14 g (88%). M.p. > 300 °C. IR (KBr): $\tilde{\nu}$ = 3449 s, 3143 m, 2464 m, 1605 m, 1409 s, 1297 s, 1129 s, 1050 s, 980 vs, 802 s, 753 s, 727 vs, 702 s cm^{-1}. MS (+FAB): *m*/*z* = 993 $[M + H]^+$, 779 $[Er(TPP)]^+$ for ^{167}Er. ESI-HRMS (+ve mode, in CH_3OH): *m*/*z* = 992.2815 {$[M + H]^+$, $C_{53}H_{39}BN_{10}Er$ requires 992.2755}.

[Er(TMPP)(Tp^H)] (8): Solution **B** (5.0 mL), H_2TMPP (0.12 g, 0.17 mmol) and KT^H_P (0.10 g, 0.40 mmol) were used. Yield: 0.14 g (80%). M.p. > 300 °C. IR (KBr): $\tilde{\nu}$ = 3452 m, 2966 m, 2831 w, 2459 w, 1606 m, 1521 s, 1509 s, 1296 s, 1250 vs, 1176 vs, 1050 m, 988 s, 804 s, 730 s, 597 m cm^{-1}. MS (+FAB): *m*/*z* = 1113 $[M + H]^+$, 899 $[Er(TMPP)]^+$ for ^{167}Er. ESI-HRMS (+ve mode, in CH_3OH): *m*/*z* = 1112.3141 {$[M + H]^+$, $C_{57}H_{47}BN_{10}O_4Er$ requires 1112.3177}.

[Er(TTP)(Tp^H)] (9): Solution **B** (5.0 mL), H_2TTP (0.12 g, 0.18 mmol) and KT^H_P (0.10 g, 0.40 mmol) were used. Yield: 0.16 g (86%). M.p. > 300 °C. IR (KBr): $\tilde{\nu}$ = 3441 m, 2929 w, 2459 w, 1528 s, 1409 m, 1331 s, 1296 m, 1128 vs, 1049 s, 990 vs, 800 s, 728 s cm^{-1}. MS (+FAB): *m*/*z* = 1046 $[M + H]^+$, 833 $[Er(TTP)]^+$ for ^{167}Er. ESI-HRMS (+ve mode, in CH_3OH): *m*/*z* = 1048.3425 {$[M + H]^+$, $C_{57}H_{47}BN_{10}Er$ requires 1048.3381}.

[Er(TBPP)(Tp^H)] (10): Solution **B** (5.0 mL), H_2TBPP (0.11 g, 0.12 mmol) and KT^H_P (0.10 g, 0.40 mmol) were used. Yield: 0.14 g (91%). M.p. > 300 °C. IR (KBr): $\tilde{\nu}$ = 3449 s, 2919 m, 2454 w, 1636 m, 1479 m, 1388 m, 1295 vs, 1131 s, 1071 m, 1049 s, 989 vs, 804 m, 727 m, 462 m cm^{-1}. MS (+FAB): *m*/*z* = 1305 $[M + H]^+$, 1091 $[Er(TBPP)]^+$ for ^{79}Br and ^{167}Er. ESI-HRMS (+ve mode, in

Table 3. Crystallographic data for compounds **1**, **5** and **7**

Compound	**1**·2$CHCl_3$	**5**·$CHCl_3$·CH_3OH	**7**·2$CHCl_3$
Empirical formula	$C_{55}H_{40}BCl_6N_{10}Yb$	$C_{55}H_{39}BCl_7N_{10}OYb$	$C_{55}H_{40}BCl_6ErN_{10}$
Molecular weight	1237.52	1287.96	1231.74
Crystal size [mm]	0.40 × 0.20 × 0.18	0.80 × 0.60 × 0.50	0.50 × 0.30 × 0.20
Crystal system	Monoclinic	Monoclinic	Monoclinic
Space group	$P2_1/n$	$P2_1/c$	$P2_1/n$
a [Å]	18.5807(14)	14.0166(11)	18.5620(10)
b [Å]	14.7805(11)	27.385(2)	14.8096(8)
c [Å]	19.4796(15)	15.4285(12)	19.4955(11)
β [°]	98.8320(10)	114.0270(10)	98.8120(10)
V [Å^3]	5286.3(7)	5408.9(7)	5296.0(5)
Z	4	4	4
$D_{calcd.}$ [g cm^{-3}]	1.555	1.575	1.545
T [K]	293	293	293
μ(Mo-K_α) [mm^{-1}]	2.121	2.125	1.936
F(000)	2468	2544	2460
θ range [°]	1.65−27.50	1.76−27.51	1.73−27.51
Reflections collected	30049	30928	30301
Independent reflections	11829	12119	11818
R_{int}	0.0290	0.0233	0.0216
GOF on F^2	0.949	1.064	1.064
$R1$, $wR2$ [$I > 2\sigma(I)$][a]	0.0343, 0.0866	0.0419, 0.1188	0.0316, 0.0832
$R1$, $wR2$ (all data)	0.0524, 0.0922	0.0542, 0.1281	0.0428, 0.0877

[a] $R1 = \Sigma||F_o| - |F_c||/\Sigma|F_o|$; $wR2 = [\Sigma w(|F_o^2| - |F_c^2|)^2/\Sigma w|F_o^2|^2]^{1/2}$.

CH_3OH): m/z = 1229.9271 {$[M - HBr]^+$, $C_{53}H_{34}BN_{10}Br_3Er$ requires 1311.9261}.

[Er(TCPP)(Tp^H)] (11): Solution **B** (5.0 mL), H_2TCPP (0.12 g, 0.17 mmol) and KT_P^H (0.10 g, 0.40 mmol) were used. Yield: 0.16 g (89%). M.p. > 300 °C. IR (KBr): ṽ = 3448 m, 2459 m, 2360 w, 1647 m, 1478 s, 1409 m, 1300 s, 1090 s, 1050 s, 1003 s, 800 s, 760 m, 727 m, 496 m cm^{-1}. MS (+FAB): m/z = 1129 $[M + H]^+$, 915 $[Er(TCPP)]^+$ for ^{35}Cl and ^{167}Er. ESI-HRMS (+ve mode, in CH_3OH): m/z = 1128.1289 {$[M + H]^+$, $C_{53}H_{35}BN_{10}Cl_4Er$ requires 1128.1196}.

[Er(TFPP)(Tp^H)] (12): Solution **B** (5.0 mL), H_2TFPP (0.11 g, 0.17 mmol) and KT_P^H (0.10 g, 0.40 mmol) were used. Yield: 0.17 g (89%). M.p. > 300 °C. IR (KBr): ṽ = 3431 m, 2960 m, 2453 w, 1605 m, 1508 vs, 1409 m, 1295 s, 1221 s, 1158 vs, 1052 s, 988 s, 800 vs, 726 m, 591 m cm^{-1}. MS (+FAB): m/z = 1065 $[M + H]^+$, 851 $[Er(TFPP)]^+$ for ^{167}Er. ESI-HRMS (+ve mode, in CH_3OH): m/z = 1064.2468 {$[M + H]^+$, $C_{53}H_{35}BN_{10}F_4Er$ requires 1064.2378}.

X-ray Crystallography. Pertinent crystallographic data and other experimental details are summarized in Table 3. Crystals suitable for X-ray diffraction studies were grown by slow evaporation of solutions of the respective compounds in chloroform/methanol. No decay in intensity was encountered during the data collection. Intensity data for **1**, **5** and **7** were collected at 293 K on a Bruker Axs SMART 1000 CCD area-detector diffractometer using graphite-monochromated Mo-K_α radiation (λ = 0.71073 Å). The collected frames were processed with the software SAINT,[34] and an absorption correction was applied (SADABS)[35] to the collected reflections. The space groups of each crystal were determined from the systematic absences and Laue symmetry checks and confirmed by successful refinement of the structures. The structures of all compounds were solved by direct methods (SHELXTL)[36] and refined against F^2 by full-matrix least-squares analyses. All non-hydrogen atoms were refined anisotropically. Hydrogen atoms were generated in their idealized positions and allowed to ride on their respective parent carbon atoms.

CCDC-213538 (**1**), -213539 (**5**) and -213540 (**7**) contain the supplementary crystallographic data for this paper. These data can be obtained free of charge at www.ccdc.cam.ac.uk/conts/retrieving.html or from the Cambridge Crystallographic Data Centre, 12 Union Road, Cambridge CB2 1EW, UK [Fax: (internat.) + 44-1223/336-033; E-mail: deposit@ccdc.cam.ac.uk].

Acknowledgments

W.-K. Wong thanks the Hong Kong Baptist University (FRG/01-02/II-40) and the Hong Kong Research Grants Council (HKBU 2023/00P) for financial support.

[1] A. Beeby, R. S. Dickins, S. Faulkner, D. Parker, J. A. G. Williams, *Chem. Commun.* **1997**, 1401−1402.
[2] S. I. Klink, P. Oude Alink, L. Grave, F. G. A. Peters, J. W. Hofstraat, F. Geurts, F. C. J. M. van Veggel, *J. Chem. Soc., Perkin Trans. 2* **2001**, 363−372.
[3] M. H. V. Werts, J. W. Verhoeven, J. W. Hofstraat, *J. Chem. Soc., Perkin Trans. 2* **2000**, 433−439.
[4] M. H. V. Werts, J. W. Hofstraat, F. A. J. Geurts, J. W. Verhoeven, *Chem. Phys. Lett.* **1997**, *276*, 196−201.
[5] S. I. Klink, H. Keizer, F. C. J. M. van Veggel, *Angew. Chem.* **2000**, *112*, 4489−4491; *Angew. Chem. Int. Ed.* **2000**, *39*, 4319−4321.
[6] M. H. V. Werts, R. H. Woudenberg, P. G. Emmerink, R. van Gassel, J. W. Hofstraat, J. W. Verhoeven, *Angew. Chem.* **2000**, *112*, 4716−4718; *Angew. Chem. Int. Ed.* **2000**, *39*, 4542−4544.
[7] J. X. Meng, K. F. Li, J. Yuan, L. L. Zhang, W. K. Wong, K. W. Cheah, *Chem. Phys. Lett.* **2000**, *332*, 313−318.
[8] [8a] W. D. Horrocks Jr., J. P. Bolender, W. D. Smith, R. M. Supkowski, *J. Am. Chem. Soc.* **1997**, *119*, 5972−5973. [8b] G. F. de Sá, O. L. Malta, C. de Mello Donegá, A. M. Simas, R. L. Longo, P. A. Santa-Cruz, E. F. da Silva Jr., *Coord. Chem. Rev.* **2000**, *196*, 165−195. [8c] F. R. G. e Silva, O. L. Malta, C. Reinhard, H.-U. Güdel, C. Piguet, J. E. Moser, J.-C. G. Bünzli, *J. Phys. Chem. A* **2002**, *106*, 1670−1677. [8d] G. A. Hebbink, L. Grave, L. A. Woldering, D. N. Reinhoudt, F. C. J. M. van Veggel, *J. Phys. Chem. A* **2003**, *107*, 2483−2491.

[9] W. T. Carnall, *Handbook on the Physics and Chemistry of Rare Earths* (Ed.: K. A. Gschneidner, Jr., L. Eyring), Elsevier, Amsterdam, **1987**, vol. 3, p. 171.
[10] M. P. Oude Wolbers, F. C. J. M. van Veggel, B. H. M. Snellink-Ruel, J. W. Hofstraat, F. A. J. Geurts, D. N. Reinhoudt, *J. Chem. Soc., Perkin Trans. 2* **1998**, 2141−2150.
[11] C. P. Wong, R. F. Venteicher, W. D. Horrocks Jr., *J. Am. Chem. Soc.* **1974**, *96*, 7149−7150.
[12] G. A. Spyroulias, A. G. Coutsolelos, *Polyhedron* **1995**, *14*, 2483−2490.
[13] W. D. Horrocks Jr., R. F. Venteicher, C. A. Spilburg, B. L. Vallee, *Biochem. Biophys. Res. Commun.* **1975**, *64*, 317−322.
[14] W. D. Horrocks Jr., C. P. Wong, *J. Am. Chem. Soc.* **1976**, *98*, 7157−7162.
[15] W. D. Horrocks Jr., E. G. Hove, *J. Am. Chem. Soc.* **1978**, *100*, 4386−4392.
[16] M. I. Gaiduk, V. V. Grigoryants, A. F. Mironov, V. D. Rumyantseva, V. I. Chissov, G. M. Sukhin, *J. Photochem. Photobiol. B* **1990**, *7*, 15−20.
[17] Y. Korovin, Z. Zhilina, N. Kuzmin, S. Vodzinsky, Y. Ishkov, *J. Porphyrins Phthalocyanines* **2001**, *5*, 481−485.
[18] W. K. Wong, A. X. Hou, J. P. Gou, H. S. He, L. L. Zhang, W. Y. Wong, K. F. Li, K. W. Cheah, T. C. W. Mak, *J. Chem. Soc., Dalton Trans.* **2001**, 3092−3098.
[19] H. S. He, Z. X. Zhao, W. K. Wong, K. F. Li, J. X. Meng, K. W. Cheah, *Dalton Trans.* **2003**, 980−986.
[20] W. K. Wong, L. L. Zhang, W. T. Wong, F. Xue, T. C. W. Mak, *J. Chem. Soc., Dalton Trans.* **1999**, 615−622.
[21] W. K. Wong, L. L. Zhang, W. T. Wong, F. Xue, T. C. W. Mak, *J. Chem. Soc., Dalton Trans.* **1999**, 3053−3062.
[22] A. D. Adler, F. R. Longo, J. D. Finarelli, J. Goldmacher, J. Assour, I. Korsakoff, *J. Org. Chem.* **1967**, *32*, 476−477.
[23] K. Kalyanasundaram, *Photochemistry of Polypyridine and Porphyrin Complexes*, Academic Press, London, **1992**, p. 376.
[24] M. Gouterman, *The Porphyrins* (Ed.: D. Dolphin), Academic Press, New York, **1978**, vol. III, chapter 1.
[25] L. R. Milgrom, *The Colours of Life: An Introduction to The Chemistry of Porphyrins and Related Compounds*, Oxford University Press, Oxford, **1997**, p. 85.
[26] Z. Katona, A. Grofcsik, P. Baranyai, I. Bitter, G. Grabner, M. Kubinyi, T. Vidoczy, *J. Mol. Struct.* **1998**, *450*, 41−45.
[27] S. C. Jeoung, D. Kim, K. H. Ahn, D. W. Cho, M. Yoon, *Chem. Phys. Lett.* **1995**, *241*, 533−539.
[28] D. J. Quimby, F. R. Longo, *J. Am. Chem. Soc.* **1974**, *97*, 5111−5117.
[29] M. M. Nei, A. D. Adler, *J. Am. Chem. Soc.* **1974**, *97*, 5107−5111.
[30] N. Sabbatini, M. Guardigli, J.-M. Lehn, *Coord. Chem. Rev.* **1993**, *123*, 201−228 and references cited therein.
[31] A. Beeby, I. M. Clarkson, R. S. Dichins, S. Faulkner, D. Parker, L. Royle, A. S. de Sousa, J. A. G. Williams, M. Woods, *J. Chem. Soc., Perkin Trans. 2* **1999**, 493−504.
[32] C. A. Parker, W. T. Rees, *Analyst (London)* **1960**, *85*, 587−600.
[33] K. Nakamaru, *Bull. Chem. Soc. Jpn.* **1982**, *55*, 1639−1640.
[34] *SAINT*, Reference manual, Siemens Energy and Automation, Madison, WI, **1994−1996**.
[35] G. M. Sheldrick, *SADABS, Empirical Absorption Correction Program*, University of Göttingen, Germany, **1997**.
[36] G. M. Sheldrick, *SHELXTL*™ Reference manual, version 5.1, Siemens, Madison, WI, **1997**.

Received July 28, 2003
Early View Article
Published Online January 19, 2004

